Journal of Saudi Chemical Society (2016) xxx, xxx–xxx

King Saud University

Journal of Saudi Chemical Society

www.ksu.edu.sa
www.sciencedirect.com

ORIGINAL ARTICLE

Synthesis, structural studies and antituberculosis evaluation of new hydrazone derivatives of quinoline and their Zn(II) complexes

Mustapha C. Mandewale [a,*], Bapu Thorat [a], Y. Nivid [c], Ram Jadhav [a], Aarti Nagarsekar [a], Ramesh Yamgar [b]

[a] *P.G. and Research Centre, Department of Chemistry, Government of Maharashtra, Ismail Yusuf College of Arts, Science and Commerce, Jogeshwari (East), Mumbai 400 060, India*
[b] *Department of Chemistry, Chikitsak Samuha's Patkar-Varde College of Arts, Science and Commerce, Goregaon (West), Mumbai 400 062, India*
[c] *Terna Medical College, Nerul, Navi Mumbai 400706, India*

Received 5 February 2016; revised 2 April 2016; accepted 8 April 2016

KEYWORDS

Quinoline;
Hydrazone;
Metal complex;
Antituberculosis;
Fluorescence

Abstract The quinoline hydrazone ligands were synthesized through multi-step reactions. The 2-hydroxy-3-formylquinoline derivatives (**1a–1c)** were prepared from acetanilide derivatives as starting materials using Vilsmeier–Haack reaction. Then the condensation of 2-hydroxy-3-formylquinoline derivatives with hydrazide derivatives (**2a–2c)** yielded quinoline hydrazone ligands (**3a–3i)**. The synthesis of a new series of Zn(II) complexes carried out by refluxing with these quinoline hydrazone ligands (**3a–3i)** is reported. The molecular structures of the ligands (**3a–3i)** and the Zn complexes were characterized by elemental analysis and spectral studies like FT-IR, ^{1}H and ^{13}C NMR, MS, UV–Visible and fluorescence. The preliminary results of antituberculosis study showed that most of the Zn(II) complexes **4a–4i** demonstrated very good antituberculosis activity while the ligands **3a–3i** showed moderate activity. Among the tested compounds **4e** and **4g** were found to be most active with minimum inhibitory concentration (MIC) of 8.00 μM and 7.42 μM respectively against *Mycobacterium tuberculosis* (H37 RV strain) ATCC No-27294 which is comparable to "first and second line" drugs used to treat tuberculosis.

1. Introduction

The extremely drug resistant tuberculosis is a worldwide public health problem in recent years. The wide spread of this disease is primarily due to the development of resistance to the existing drugs that has concerned researchers throughout the world. There is an urgent requirement of improvement in new drug

* Corresponding author. Tel.: +91 9773998405.
E-mail address: iycmustapha@gmail.com (M.C. Mandewale).
Peer review under responsibility of King Saud University.

Production and hosting by Elsevier

http://dx.doi.org/10.1016/j.jscs.2016.04.003
1319-6103

Please cite this article in press as: M.C. Mandewale et al., Synthesis, structural studies and antituberculosis evaluation of new hydrazone derivatives of quinoline and their Zn(II) complexes, Journal of Saudi Chemical Society (2016), http://dx.doi.org/10.1016/j.jscs.2016.04.003

molecules with newer targets and with an alternative mechanism of action [1,2]. It is evident from the literature that quinoline-based hydrazone scaffolds are known to exhibit excellent anti-TB properties [3–8]. This broad spectrum of biological and biochemical activities has been further aided by the synthetic flexibility of quinoline hydrazones, which allows the generation of a large number of structurally diverse derivatives and their metal complexes [9,10]. Further, various types of hydrazones have attracted continued interest in the medicinal field due to their broad-spectrum biological activities [11]. Among the ligand systems, quinoline hydrazone derivatives are highly important because, these ligands developed due to their diverse chelating ability, structural flexibility and pharmacological activities like antitumoural, antifungal, antibacterial, antituberculosis, antimalarial, and antiviral [12,13].

Zinc is an important trace element in human beings, and is participating in several biological processes in the form of complexes with proteins and nucleic acids. Moreover, Zn(II) ions are important for the expression of genetic information and structural maintenance of chromatin [14–17]. Numerous examples of Zn(II) complexes have been investigated for their significant antibacterial activity [18].

Recently it is reported that quinoline hydrazones and their Zn(II) complexes showed significant activity against the *Mycobacterium tuberculosis* strain, at low micromolar levels [19,20,10]. Based on these facts, supported by literature and in continuation of our research for new antituberculosis agents [21,22], we have undertaken research studies on synthesis and biological screening of some new quinoline hydrazone derivatives and their Zn(II) complexes shown in Fig. 1.

2. Experimental

The melting points of synthesized compounds were determined in open capillary tubes and are uncorrected. UV–Visible spectra were obtained on Shimadzu UV-1800 spectrophotometer. The fluorescence spectra were recorded on a spectrofluorophotometer Shimadzu RF-5301pc and equipped with quartz cuvette of 1 cm path length. Infrared spectra were measured with KBr disc on a FTIR-7600 Lambda Scientific Pty. Ltd. in the range 4000–400 cm^{-1}. Mass spectra were performed on BRUKER ESQUIRE HCT spectrometer. ^1H NMR and ^{13}C NMR spectra were recorded on Varian-NMR-Mercury 300 MHz instruments in DMSO-d_6 using tetramethylsilane (TMS) as an internal standard; chemical shifts are reported as δ ppm units. The elemental analyses were done at the SAIF, IIT Mumbai, India. The DSC–TGA analysis was carried out on Universal V4.5A TA instrument. Thin-layer chromatography (TLC) was performed on pre-coated TLC sheets of silica gel 60 F254 (Merck, Darmstadt, Germany), visualized by long- and short-wavelength UV lamps. Chromatographic purifications were performed on Merck silica gel (60−120 mesh).

2.1. General procedure for preparation of hydrazones *3a–3i* and Zn(II) complexes *4a–4i*

A mixture of compound **1a–1c** (0.01 mol) and appropriate hydrazide derivatives **2a–2c** (0.01 mol) in 10 mL of ethanol was stirred for 30 min at 60 °C. Completion of reaction is checked with TLC. The reaction mixture was allowed to cool down to room temperature and the solid formed was filtered, dried and recrystallized from ethanol to afford hydrazones **3a–3i**. Their structures are represented in Table 1 and Fig. 2.

A solution of Zinc chloride dissolved in ethanol was added gradually to a stirred ethanolic solution of the hydrazone ligand **3a–3i** in the molar ratio 1:2. The reaction mixture was further stirred for 2–4 h at 60 °C. The reaction mixture was allowed to cool down to room temperature and the solid formed was filtered, and washed several times with water. Finally, the complexes **4a–4i** were washed with diethyl ether and dried in vacuum desiccators over anhydrous $CaCl_2$. Probable structures are presented in Table 2 and Fig. 2.

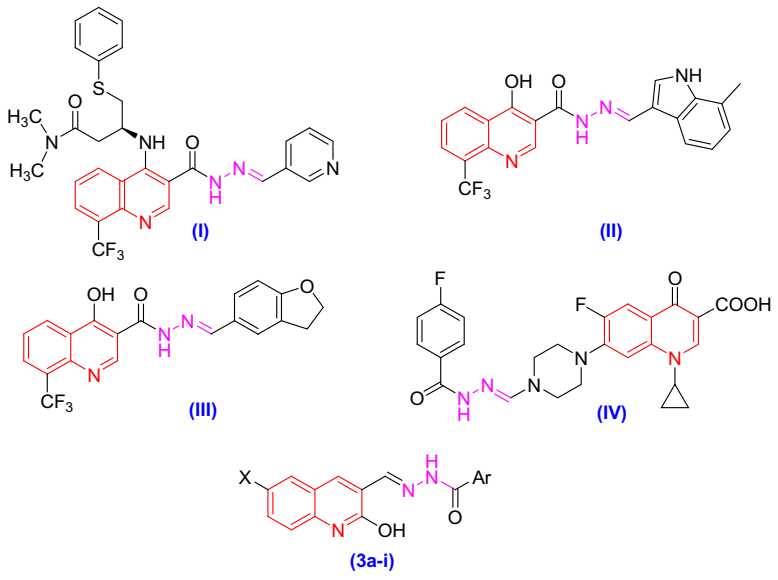

Figure 1 Previously reported quinoline hydrazones as anti-tuberculosis agents and synthesized compounds.

Table 1 Structures of hydrazones **3a**–**3i.**

Entry	Hydrazide	Hydrazone [3]	Yield (%)
a	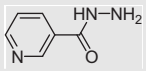	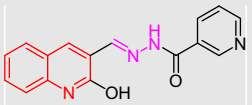	89
b	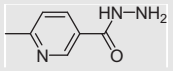	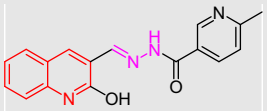	86
c	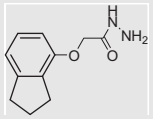	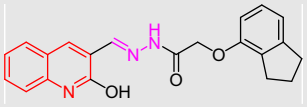	90
d	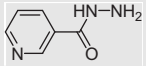	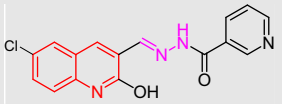	91
e	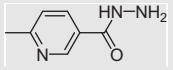	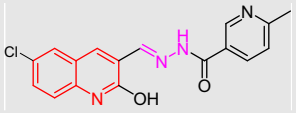	86
f	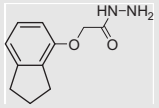	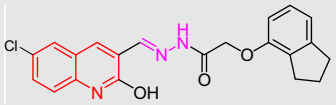	88
g	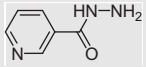	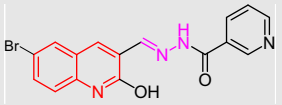	94
h	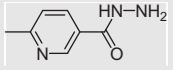	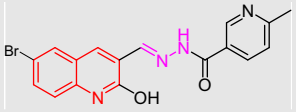	89
i	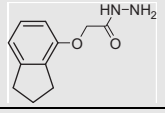	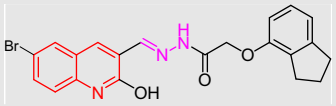	87

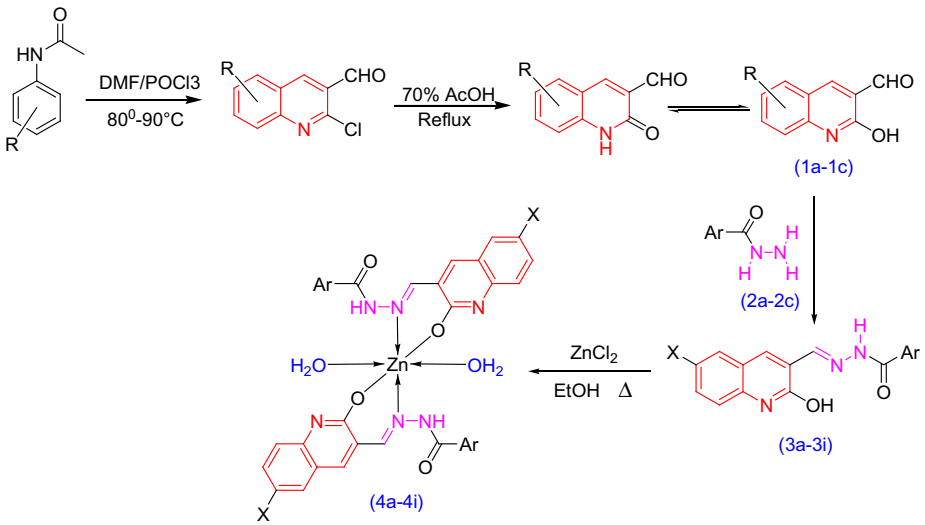

Figure 2 Preparation of hydrazones **3a**–**3i** and Zn(II) complexes **4a**–**4i**.

Table 2 Preparation of Zn(II) complexes **4a**–**4i**.

Entry	Complex	Colour	Entry	Complex	Colour
4a	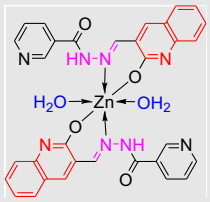	Yellow	**4f**	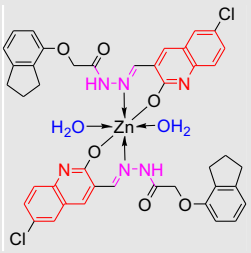	Yellow
4b	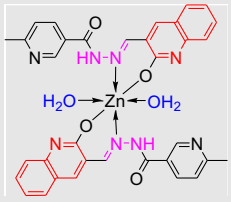	Yellow	**4g**	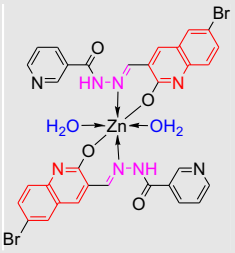	Yellow
4c	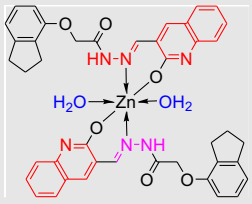	Yellow	**4h**	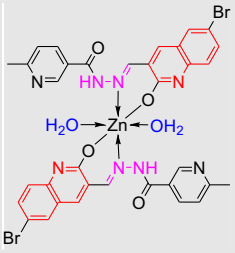	Yellow
4d	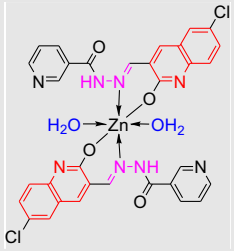	Yellow	**4i**	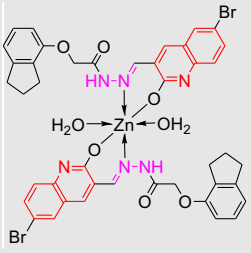	Yellow
4e	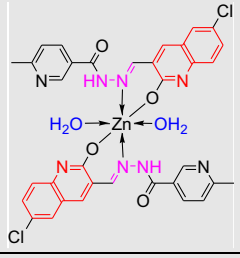	Yellow			

*2.1.1. N′-[(E)-(2-hydroxyquinolin-3-yl)methylidene]pyridine-3-carbo hydrazide [**3a**]*

M.P.: 296 °C; colour: pale yellow; MS [M + 2]: 294.80; FTIR (KBr cm^{-1}): 3237 (phenolic—OH), 3093 (N—H amide), 1662 (C═O amide), 1596 (imine —CH═N—), 1486 (phenolic C—O); ^{1}H NMR (DMSO-d_6) δ: 7.19–7.24 (m, 1H), 7.33–7.36 (m, 1H), 7.52–7.58 (m, 2H), 7.85–7.88 (d, 1H), 8.27–8.29 (d, 1H), 8.49 (s, 1H), 8.72–8.76 (m, 2H), 9.09 (s, 1H), 12.02 (s, 1H), 12.13 (s, 1H); ^{13}C NMR (DMSO-d_6) δ: 124.5, 125.9, 127.1, 128.0, 128.7, 128.8, 129.0, 130.5, 130.2, 134.5, 147.2, 147.1, 147.9, 149.8 (C═N), 160.8 (C—OH), 163.1 (—C═O); elemental analysis [$C_{16}H_{12}N_4O_2$] observed (calculated): C 65.79% (65.75%), H 4.11% (4.14%), N 19.22% (19.17%).

*2.1.2. N′-[(E)-(2-hydroxyquinolin-3-yl)methylidene]-6-methylpyridine-3-carbohydrazide [**3b**]*

M.P.: 286 °C; colour: faint yellow; MS [M + H]: 307.02; FTIR (KBr cm^{-1}): 3453 (phenolic—OH), 3237 (N—H amide), 3048 (aromatic C—H), 1660 (C═O amide), 1600 (imine —CH═N—), 1432 (phenolic C—O); ^{1}H NMR (DMSO-d_6) δ: 2.55 (s, 1H), 7.19–7.24 (m, 1H), 7.33–7.43 (m, 2H), 7.52–7.56 (m, 1H), 7.85–7.88 (m, 1H), 8.17–8.19 (m, 1H), 8.48 (s, 1H),

Please cite this article in press as: M.C. Mandewale et al., Synthesis, structural studies and antituberculosis evaluation of new hydrazone derivatives of quinoline and their Zn(II) complexes, Journal of Saudi Chemical Society (2016), http://dx.doi.org/10.1016/j.jscs.2016.04.003

8.71 (s, 1H), 8.97 (s, 1H), 12.04 (s, 1H), 12.07 (s, 1H); ^{13}C NMR (DMSO-d_6) δ: 23.6 (—CH_3), 121.9, 125.6, 126.1, 128.0, 128.4, 128.8, 128.9, 129.2, 130.8, 130.9, 145.7, 147.5, 149.0 (C═N), 158.1 (C—OH), 161.5 (—C═O); elemental analysis [$C_{17}H_{14}N_4O_2$] observed (calculated): C 66.57% (66.66%), H 4.50% (4.61%), N 18.22% (18.29%).

*2.1.3. 2-[(2,3-dihydro-1H-inden-4-yl)oxy]-N′-[(E)-(2-hydroxyquinolin-3-yl)methylidene]aceto hydrazide [**3c**]*

M.P.: above 300 °C; colour: faint yellow; MS [M + 1]: 362.00; FTIR (KBr cm^{-1}): 3210 (phenolic—OH), 3149 (N—H amide), 2952 (aromatic C—H), 2846 (aliphatic C—H), 1656 (C═O amide), 1614 (imine —CH═N—), 1427 (phenolic C—O); ^{1}H NMR (DMSO-d_6) δ: 1.98–2.01 (m, 2H), 2.81–2.86 (m, 4H), 4.64 (s, 2H), 6.61–6.63 (m, 1H), 6.79–6.82 (m, 1H), 7.04–7.07 (m, 1H), 7.16–7.21 (m, 1H), 7.29–7.32 (m, 1H), 7.48–7.51 (m, 1H), 7.72–7.75 (m, 1H), 8.23 (s, 1H), 8.40–8.42 (m, 1H), 11.70 (s, 1H), 12.03 (s, 1H); ^{13}C NMR (DMSO-d_6) δ: 25.5 (aliphatic CH_2), 29.7 (aliphatic CH_2), 32.5 (aliphatic CH_2), 66.8 (aliphatic —CH_2—O—), 113.7, 125.1, 126.4, 127.1, 128.0, 128.7, 128.8, 129.0, 130.3, 130.8, 135.1, 138.5, 146.1, 148.2 (C═N), 155.8 (aromatic —C—O—), 160.5 (C—OH), 167.5 (—C═O); elemental analysis [$C_{21}H_{19}N_3O_3$]: observed (calculated): C 69.87% (69.79%), H 5.34% (5.30%), N 11.56% (11.63%).

*2.1.4. N′-[(E)-(6-chloro-2-hydroxyquinolin-3-yl)methylidene] pyridine-3-carbohydrazide [**3d**]*

M.P.: 298 °C; colour: yellow; MS [M + 2]: 328.39; FTIR (KBr cm^{-1}): 3214 (phenolic—OH), 3072 (N—H amide), 1656 (C═O amide), 1617 (imine —CH═N—), 1417 (phenolic C—O); ^{1}H NMR (DMSO-d_6) δ: 7.33–7.36 (m, 1H), 7.55–7.58 (m, 2H), 8.03 (s, 1H), 8.27–8.29 (m, 1H), 8.49 (s, 1H), 8.70–8.77 (m, 2H), 8.09 (s, 1H), 12.17 (s, 1H), 12.19 (s, 1H); ^{13}C NMR (DMSO-d_6) δ: 123.5, 125.1, 126.6, 128.2, 130.2, 130.3, 130.5, 130.7, 132.3, 134.2, 146.1, 147.1, 148.2, 149.8 (C═N), 160.5 (C—OH), 162.8 (—C═O); elemental analysis [$C_{16}H_{11}ClN_4O_2$]: observed (calculated): C 58.91% (58.82%), H 3.44% (3.39%), N 17.23% (17.15%).

*2.1.5. N′-[(E)-(6-chloro-2-hydroxyquinolin-3-yl)methylidene]-6-methylpyridine-3-carbohydrazide [**3e**]*

M.P.: 298 °C; colour: yellow; MS [M—H]: 339.36; FTIR (KBr cm^{-1}): 3237 (phenolic—OH), 3087 (N—H amide), 3006 (aromatic C—H), 2875 (aliphatic C—H), 1660 (C═O amide), 1604 (imine —CH═N—), 1415 (phenolic C—O); ^{1}H NMR (300 MHz, DMSO-d_6) δ: 2.55 (s, 3H), 7.32–7.42 (m, 2H), 7.55–7.57 (m, 1H), 8.01 (s, 1H), 8.16–8.19 (m, 1H), 8.47 (s, 1H), 8.69 (s, 1H), 8.97 (s, 1H), 12.09 (s, 1H), 12.14 (s, 1H); ^{13}C NMR (DMSO-d_6) δ: 23.9 (—CH_3), 122.0, 126.6, 127.1, 128.0, 128.6, 128.7, 128.8, 129.0, 130.5, 130.6, 146.1, 147.2, 147.9, 151.4 (C═N), 161.5 (C—OH), 163.0 (—C═O); elemental analysis [$C_{17}H_{13}ClN_4O_2$]: observed (calculated): C 59.99% (59.92%), H 3.91% (3.85%), N 16.51% (16.44%).

*2.1.6. N′-[(E)-(6-chloro-2-hydroxyquinolin-3-yl)methylidene]-2-[(2,3-dihydro-1H-inden-4-yl)oxy]acetohydrazide [**3f**]*

M.P.: > 300 °C; colour: yellow; MS [M + 2]: 397.63; FTIR (KBr cm^{-1}): 3185 (phenolic—OH), 3052 (N—H amide), 2921 (aromatic C—H), 2842 (aliphatic C—H), 1662 (—C═O amide), 1616 (imine —CH═N—), 1415 (C—O); ^{1}H NMR (DMSO-d_6) δ: 2.01 (m, 2H), 2.84–2.86 (m, 4H), 4.67 (s, 2H), 6.62–6.65 (m, 1H), 6.82–6.84 (m, 1H), 7.07 (m, 1H), 7.31–7.34 (m, 1H), 7.55–7.58 (m, 1H), 7.90 (m, 1H), 8.23 (s, 1H), 8.42–8.45 (m, 1H), 11.77 (m, 1H), 12.18 (s, 1H); ^{13}C NMR (DMSO-d_6) δ: 25.1 (aliphatic CH_2), 29.2 (aliphatic CH_2), 31.6 (aliphatic CH_2), 65.8 (aliphatic —CH_2—O—), 113.7, 124.7, 125.0, 125.6, 127.9, 130.3, 130.5, 130.7, 130.9, 133.5, 135.2, 137.6, 146.1, 148.4 (C═N), 154.7 (aromatic —C—O—), 161.2 (C—OH), 167.3 (—C═O); elemental analysis [$C_{21}H_{18}ClN_3O_3$]: observed (calculated): C 63.79% (63.72%), H 4.50% (4.58%), N 10.57% (10.62%).

*2.1.7. N′-[(E)-(6-bromo-2-hydroxyquinolin-3-yl)methylidene] pyridine-3-carbohydrazide [**3g**]*

M.P.: 287 °C; colour: dark yellow; MS [M + 1]: 371.49; FTIR (KBr cm^{-1}): 3241 (phenolic—OH), 3093 (N—H amide), 2902 (aromatic C—H), 1662 (C═O amide), 1604 (imine —CH═N—1413 (phenolic C—O); ^{1}H NMR (DMSO-d_6) δ: 7.25–7.28 (m, 1H), 7.56 (m, 1H), 7.66–7.68 (m, 1H), 8.15 (s, 1H), 8.25 (m, 1H), 8.46 (s, 1H), 8.68–8.76 (m, 2H), 9.07 (s, 1H), 12.15 (s, 2H); ^{13}C NMR (DMSO-d_6) δ: 118.1, 124.9, 126.6, 128.1, 130.1, 130.4, 130.5, 130.7, 133.1, 133.8, 145.1, 146.2, 147.5, 149.7 (C═N), 162.1 (C—OH), 163.2 (—C═O); elemental analysis [$C_{16}H_{11}BrN_4O_2$]: observed (calculated): C 51.82% (51.77%), H 3.06% (2.99%), N 15.01% (15.09%).

*2.1.8. N′-[(E)-(6-bromo-2-hydroxyquinolin-3-yl)methylidene]-6-methylpyridine-3-carbohydrazide [**3h**]*

M.P.: > 300 °C; colour: yellow; MS [M +]: 385.59; FTIR (KBr cm^{-1}): 3214 (phenolic—OH), 3070 (N—H amide), 2838 (aliphatic C—H), 1656 (C═O amide), 1612 (imine —CH═N—), 1473 (phenolic C—O); ^{1}H NMR (DMSO-d_6) δ: 2.55 (s, 3H), 7.27–7.30 (m, 1H), 7.41–7.43 (m, 1H), 7.67–7.70 (m, 1H), 8.16 (m, 2H), 8.47 (s, 1H), 8.70 (s, 1H), 8.98 (s, 1H), 12.12 (s, 1H), 12.17 (s, 1H); ^{13}C NMR (DMSO-d_6) δ: 22.8 (—CH_3), 116.6, 121.9, 126.6, 127.9, 129.3, 130.1, 130.3, 130.5, 130.8, 133.4, 142.1, 144.2, 149.8, 152.1 (C═N), 160.7 (C—OH), 163.1 (—C═O); elemental analysis [$C_{17}H_{13}BrN_4O_2$]: observed (calculated): C 52.91% (53.00%), H 3.42% (3.40%), N 14.59% (14.54%).

*2.1.9. N′-[(E)-(6-bromo-2-hydroxyquinolin-3-yl)methylidene]-2-[(2,3-dihydro-1H-inden-4-yl)oxy]acetohydrazide [**3i**]*

M.P.: > 300 °C; colour: faint yellow; MS [M + 2]: 441.56; FTIR (KBr cm^{-1}): 3185 (phenolic—OH), 3045 (N—H amide), 2925 (aromatic C—H), 2840 (aliphatic C—H), 1662 (C═O amide), 1612 (imine —CH═N—), 1567, 1479 (phenolic C—O); ^{1}H NMR (DMSO-d_6) δ: 1.99 (m, 2H), 2.81–2.84 (m, 4H), 4.65 (m, 2H), 6.61–6.63 (m, 1H), 6.80–6.82 (m, 1H), 7.05 (m, 1H), 7.23–7.26 (m, 1H), 7.63–7.66 (m, 1H), 8.00 (s, 1H), 8.20 (m, 1H), 8.50 (s, 1H), 11.75 (m, 1H), 12.15 (s, 1H); ^{13}C NMR (DMSO-d_6) δ: 25.2 (aliphatic CH_2), 29.6 (aliphatic CH_2), 32.6 (aliphatic CH_2), 66.8 (aliphatic —CH_2—O—), 113.7, 117.6, 125.0, 126.6, 127.9, 130.4, 130.6, 130.7, 130.8, 133.4, 135.1, 137.5, 146.1, 149.2 (C═N), 155.8 (aromatic —C—O—), 161.5 (C—OH), 168.5 (—C═O); elemental analysis [$C_{21}H_{18}BrN_3O_3$]: observed (calculated): C 48.52% (48.58%), H 3.32% (3.30%), N 8.14% (8.09%).

Please cite this article in press as: M.C. Mandewale et al., Synthesis, structural studies and antituberculosis evaluation of new hydrazone derivatives of quinoline and their Zn(II) complexes, Journal of Saudi Chemical Society (2016), http://dx.doi.org/10.1016/j.jscs.2016.04.003

3. Results and discussion

3.1. Chemistry

The target Zn(II) complexes 4a–4i were synthesized as depicted in Fig. 2. The first step involves the synthesis of derivatives of 2-hydroxy-3-carbaldehyde **1a**–**1c** from corresponding acetanilide derivative via a Vilsmeier–Haack reaction as previously reported [23–25]. Condensation of equimolar amounts of aldehyde **1a**–**1c** with hydrazides **2a**–**2c** in warming ethanol at 70 °C afforded hydrazones **3a**–**3i**. Elemental analyses and spectral data (FT-IR, ^{1}H and ^{13}C NMR, MS, UV–Visible and fluorescence) confirmed the structure of the products **3a**–**3i**. The FT-IR spectrum of hydrazone **3i**, as a representative example, showed strong absorption bands at 1662 and 1612 cm^{-1} due to a conjugated C═N and C═O functions, respectively. The broad peak at 3185 cm^{-1} is attributed to hydroxyl group, which is present at the 2nd position of quinoline ring. The important IR peaks and their assignments are listed in Table 3. Its ^{1}H NMR spectrum revealed, in addition to expected aromatic signals, three singlets at δ 8.50, 11.75, 12.15 ppm are assignable to the azomethine proton (─CH═N─), hydroxyl proton (─OH) and amide proton (─NH─C═O), respectively. In addition, the ^{13}C NMR spectrum of **3i** displayed three characteristic peaks at δ 149.2, 161.5, 168.5 ppm assignable to imine carbon, carbon linked to the hydroxyl group of quinoline and amide carbonyl carbon, respectively. Moreover the mass spectrum of **3i** revealed ion peak at m/z 441.56 (M + 2) corresponding molecular formula [$C_{21}H_{18}BrN_3O_3$]. In a similar manner, compounds **3a**–**3h** were prepared and characterized.

The hydrazone ligand **3a**–**3i** refluxed with $ZnCl_2$ in ethanol with molar ratio 2:1 offer Zn(II) complexes **4a**–**4i**. All metal complexes show broad peaks in the region of 3330–3517 cm^{-1} due to coordinated water molecules. The coordination mode of hadrazone with central metal ion can be explained on the basis of FTIR spectral study Table 4. The phenolic ─OH band appears at 3139–3488 cm^{-1} which disappears in IR spectra of the metal complexes, however new broad peaks have been observed at 3330–3517 cm^{-1} due to coordinated water molecules which confirms the complexation of hydrazones with central metal atom through phenolic ─OH. The low frequency region of the spectra indicated the presence of two new medium intensity bands at about 443–485 cm^{-1} due to νM─O vibrations. The IR spectra of all the metal complexes show prominent band at about 501–620 cm^{-1} due to νM─N stretching.

The magnetic study shows all Zinc(II) complexes were diamagnetic in nature. The DSC–TGA analysis was carried out to explain the thermal stability of the complexes. The thermal behaviour of the metal complex **4e** Fig. 3 was studied in the temperature range of 25–1000 °C. The TG–DTA studies of complex **4e** show that the decomposition proceeds in three steps. In the first stage, weight loss below 100 °C corresponds to the presence of the lattice cell water in the complexes. Second step involves weight loss in the temperature range 110–200 °C which is due to elimination of coordinated water. A plateau observed above 600 °C corresponds to the formation of stable Zinc oxide. Observed Zn content of the metal complexes is in good agreement with the theoretical values as shown in Table 5.

The X-ray powder diffraction data provide vital structural information of materials which do not yield single crystals of

Table 3 ^{1}H NMR signals for hydrazones **3a**–**3i** and their assignments.

Schiff base	Amide ─NH*─		Phenolic ─OH		Imine ─CH═N─	
	^{1}H NMR δ	FTIR cm^{-1}	^{1}H NMR δ	FTIR cm^{-1}	^{1}H NMR δ	FTIR cm^{-1}
3a	12.13	3093	12.02	3237	9.02	1625
3b	12.07	3237	12.04	3453	8.97	1600
3c	12.03	3210	11.70	3149	8.23	1614
3d	12.19	3072	12.17	3214	8.09	1617
3e	12.14	3087	12.09	3237	8.69	1604
3f	12.18	3052	11.77	3185	8.45	1616
3g	12.15	3093	12.15	3241	9.07	1604
3h	12.17	3070	12.12	3214	8.98	1612
3i	12.15	3045	11.75	3185	8.50	1612

Table 4 FT-IR bands for metal complexes **4a**–**4i** and their assignments.

Complex	Lattice water $\nu_{(OH)}$ cm^{-1}	Imine $\nu_{(C=N)}$ cm^{-1}	Phenolic $\nu_{(C-O)}$ cm^{-1}	$\nu_{(M-N)}$ cm^{-1}	$\nu_{(M-O)}$ cm^{-1}
4a	3446	1612	1423	576	472
4b	3517	1612	1430	572	468
4c	3370	1616	1446	611	474
4d	3394	1614	1411	555	476
4e	3330	1616	1415	570	465
4f	3378	1616	1415	570	466
4g	3394	1614	1411	532	474
4h	3374	1616	1411	535	443
4i	3300	1614	1413	540	468

Please cite this article in press as: M.C. Mandewale et al., Synthesis, structural studies and antituberculosis evaluation of new hydrazone derivatives of quinoline and their Zn(II) complexes, Journal of Saudi Chemical Society (2016), http://dx.doi.org/10.1016/j.jscs.2016.04.003

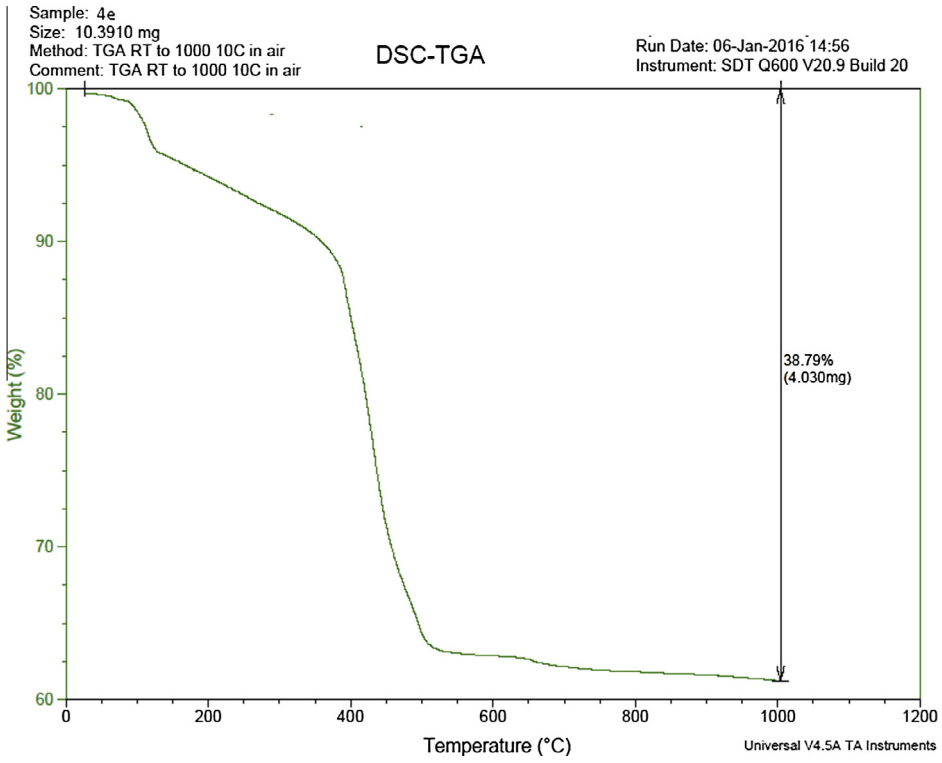

Figure 3 The DSC-TGA analysis of Zn(II) complex **4e**.

Table 5 Molar conductance (Λm) and% content of Zn in metal complexes **4a–4i.**

Complex	Molar conductance Λm (Ω^{-1} mol^{-1} cm^2)	% Zn observed (calculated)
4a	8.9	10.03 (9.56)
4b	4.1	9.06 (9.18)
4c	7.9	8.01 (7.95)
4d	6.4	8.73 (8.69)
4e	6.4	8.27 (8.37)
4f	8.8	7.39 (7.34)
4g	6.0	8.00 (7.77)
4h	8.7	7.61 (7.52)
4i	6.2	6.72 (6.67)

good quality. Single crystals of the complexes under study could not be prepared thus the powder diffraction data were acquired for structural description [26]. The X-ray diffractogram of the complex was measured in the range of 5°–80° 2θ values. The XRD pattern indicates that complex **4e** has well defined crystalline patterns, with various degrees of crystallinity Fig. 4. The average crystallite size of the complex was calculated using Scherer's formula [27,28]. The Zn(II) complex **4e** has an average crystallite size of 59 nm.

From the mathematical relation $\Lambda m = K/C$ the molar conductance of the metal complexes (Λm) can be calculated by dissolving in a proper solvent where C is the molar concentration of the metal complex solutions [29]. The metal complexes **4a–4i** were dissolved in DMF to prepare 10^{-3} M of their solutions. The molar conductivities were measured at 25 ± 2 °C. The study shows negligible molar conductance values for metal complexes **4a–4i** (4.1–8.9 Ω^{-1} mol^{-1} cm^2), indicating that the complexes are non-electrolytes. The results are represented in Table 5. From the experimental study, it is clear that practical observations are in good agreement with the theoretical values calculated for 1:2 ratio of metal:ligand stoichiometry. From the above explanation of the results of various spectroscopic details it may be concluded that the proposed geometry for the transition metal complexes with general formula $ML_2{\cdot}2H_2O$ is octahedral for Zn(II) complexes. The proposed structures are shown in Table 2.

3.2. Anti-tuberculosis evaluation

The anti-microbial effects of the new hydrazones and their Zinc complexes against *M. tuberculosis* (H37 RV strain) ATCC No-27294, were evaluated at the Department of Microbiology, Maratha Mandal's NGH Institute of Dental Sciences and Research Centre, Belgaum-590010, India. The method applied is similar to that reported by Maria and Lourenco [30]. Ciprofloxacin (MIC 9.41 μM), Pyrazinamide (MIC 25.34 μM) and Streptomycin (MIC 10.74 μM) were used as references to evaluate the potency of the synthesized compounds. As shown in Table 6 and Fig. 5, complexes **4e** and **4g** have unpredictable high anti-tuberculosis activity against *M. tuberculosis* as their MIC value is 8.00 μM and 7.42 μM respectively. All the studied samples are showing different potencies due to the effective barrier of an outer cell wall membrane of *M. tuberculosis* for entry of external substances like test compounds under this study. However, hydrazone ligands **3a–3i** showed less activity than their Zn(II) complexes **4a–4i**. This could be as a result of the metal chelates, which bear polar and nonpolar properties together; this makes them suitable for permeation to the bacterial cell. This finding indicates that

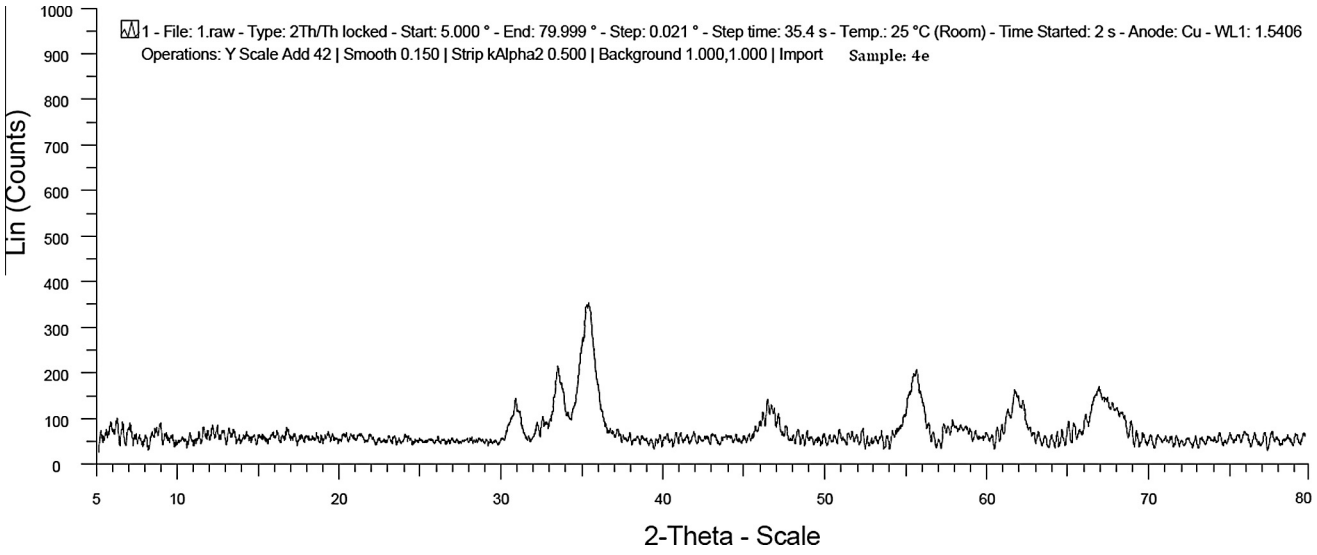

Figure 4 XRD spectra of Zn(II) complex 4e.

Table 6 Showing comparative anti-tuberculosis screening results by MIC method.

Test sample	Sample concentration in μM (MIC)	Test sample	Sample concentration in μM (MIC)
3a	171.17	**4a**	36.55
3b	163.22	**4b**	17.60
3c	69.17	**4c**	30.40
3d	76.51	**4d**	16.60
3e	73.36	**4e**	8.00
3f	126.31	**4f**	14.02
3g	67.35	**4g**	7.42
3h	32.55	**4h**	14.37
3i	56.78	**4i**	25.51
Ciprofloxacin*	9.41	Pyrazinamide*	25.34
Streptomycin*	10.74		

* Standard.

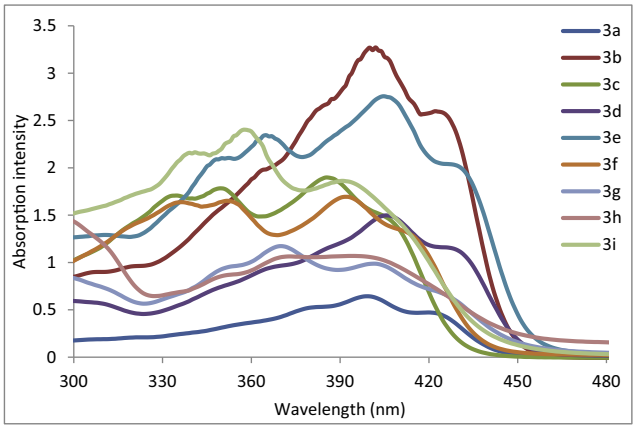

Figure 6 Electronic spectra of hydrazones (**3a**–**3i**).

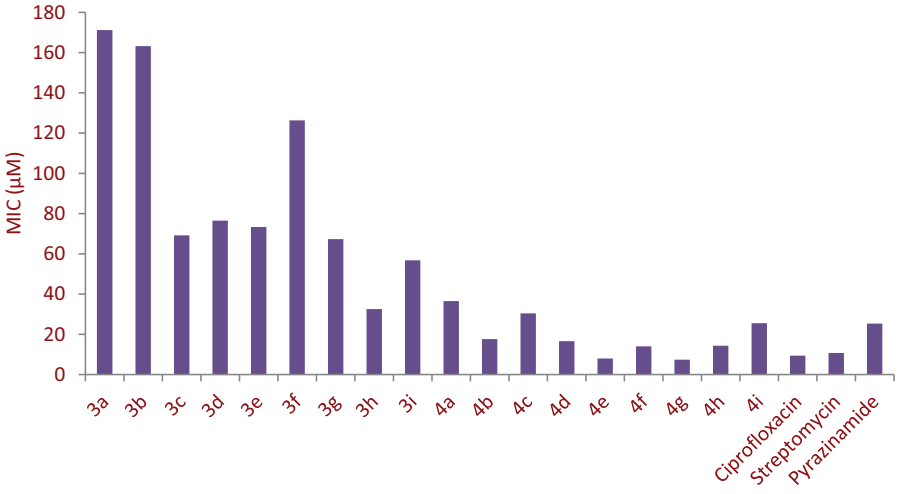

Figure 5 MIC in μM of tested compounds against *Mycobacterium tuberculosis*.

complex formation enhanced the amphiphilic properties and solubility and hence, the penetration of complex **4e** and **4g** into the cell wall of the *M. tuberculosis*, which translated into better activity. According to the Molecular Theory of Coordination metal orbital overlap with ligand orbitals this decreases the positive charge on the metal ion by accepting the electrons from donor groups of the hydrazone ligand [31,32]. Thus, the donation of the electrons from ligand to metal also favours the increased delocalization of the π-electrons through entire coordinating rings. This results in increased lipophilicity of the metal complexes. Hence, the improved lipophilicity facilitates the transport of the complexes across the lipid cell membrane of the bacteria thus, it can block the metal binding sites on different enzymes of bacteria [33,34]. These metal complexes interact with the DNA gyrase enzyme, which is necessary for DNA multiplication step. The DNA gyrase is inhibited by metal complexes, which alter the multiplication of bacterial cells, eventually resulting in the death of the bacteria [35,36].

The observed results of the test compounds indicate the future potential for the development of metal coordination complexes to solve the limitations due to currently existing anti-tuberculosis agents to treat tuberculosis.

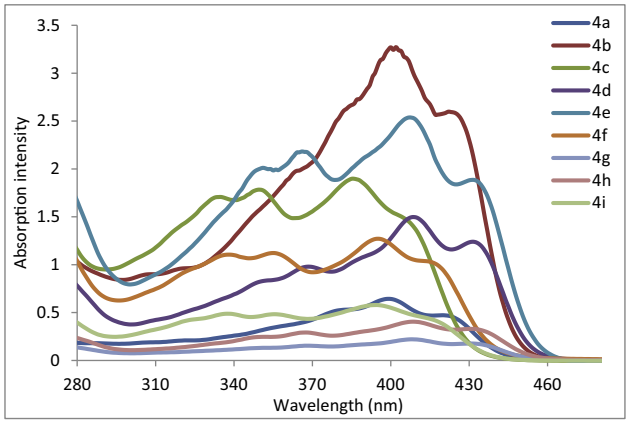

Figure 7 Electronic spectra of complexes (**4a**–**4i**).

3.3. Fluorescence study

The UV–Visible spectra of the ligands **3a**–**3i** in exhibit bands around 364–387 nm as represented in Fig. 6. The broad, intense band around 310 nm in the ligands can be assigned to intra ligand n–p* transition associated with the azomethine linkage. Fig. 7 shows this band experiences red shift in all the complexes **4a**–**4i**. The bands at around 386–408 nm are attributed to the ligand to metal charge transfer transitions.

The emission spectra of compounds **3a**–**3i** (Fig. 8) showed the emission band in the range of 440–459 nm and complexes **4a**–**4i** (Fig. 8) Table 7 showed emission band in the range of 456–485 nm. Complex formation of hydrazones induces a marked hyperchromic and bathochromic shifts. The Zn(II) complexes demonstrated intense fluorescent properties as compared to their parent ligands. The incorporation of Zn(II)

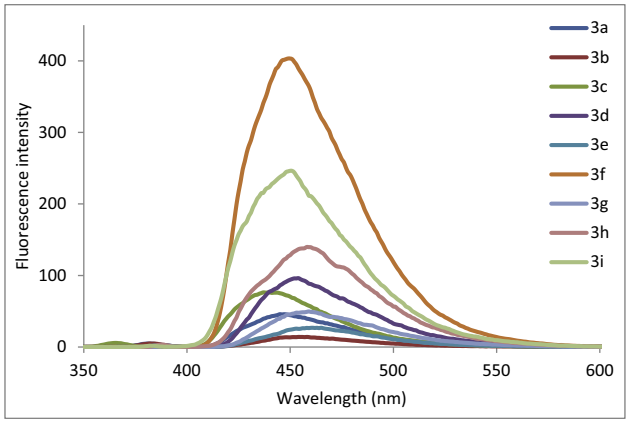

Figure 8 Fluorescence spectra of hydrazones (**3a**–**3i**).

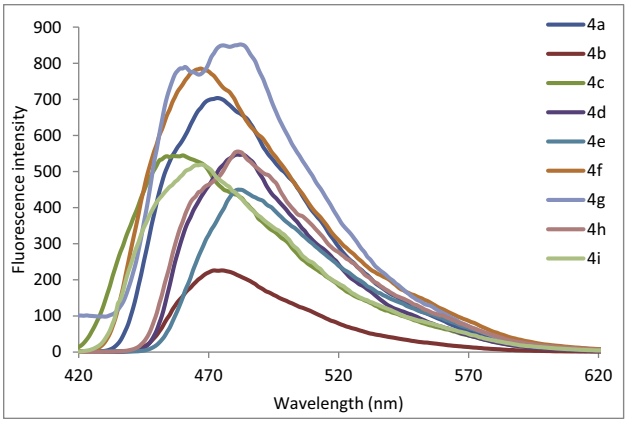

Figure 9 Fluorescence spectra of complexes (**4a**–**4i**).

Table 7 The absorption and emission wavelength with intensity.

Hydrazone	Absorption λ_{max} (intensity)	Emission λ_{max} (intensity)	Complex	Absorption λ_{max} (intensity)	Emission λ_{max} (intensity)
3a	381 (3.01)	445 (45.95)	**4a**	399 (0.64)	473 (703.56)
3b	382 (3.34)	454 (14.06)	**4b**	402 (3.27)	475 (226.04)
3c	364 (4.00)	440 (76.41)	**4c**	386 (1.89)	460 (544.80)
3d	386 (2.33)	454 (96.27)	**4d**	408 (1.49)	481 (546.76)
3e	386 (3.12)	465 (26.94)	**4e**	407 (2.53)	482 (449.49)
3f	382 (1.69)	449 (403.35)	**4f**	395 (1.27)	467 (785.49)
3g	387 (0.61)	459 (49.72)	**4g**	408 (0.221)	482 (851.90)
3h	386 (0.42)	458 (139.82)	**4h**	408 (0.405)	481 (555.31)
3i	381 (0.41)	450 (246.28)	**4i**	394 (0.579)	467 (518.87)

Please cite this article in press as: M.C. Mandewale et al., Synthesis, structural studies and antituberculosis evaluation of new hydrazone derivatives of quinoline and their Zn(II) complexes, Journal of Saudi Chemical Society (2016), http://dx.doi.org/10.1016/j.jscs.2016.04.003

effectively increases the conformational rigidity of the hydrazones and increases the fluorescence intensities of complexes **4a–4i**, which shows that it is good material in photochemical applications of these complexes (Fig. 9).

4. Conclusions

In conclusions, the objectives of the present study were to synthesize some new hydrazone derivatives with quinoline core and to perform antituberculosis analysis by blue almar method to identify the more effective compound and subsequently perform UV and fluorescence study. Most of the synthesized compounds show moderate to good antituberculosis properties. This study would pave the way for future development of more effective quinoline hydrazone analogues for biological and material applications.

Acknowledgments

The authors thank Principal and Head Department of Chemistry, Government of Maharashtra, Ismail Yusuf Arts, Science and Commerce College for providing research and library facilities. The authors also thank Dr. Kishore Bhat of Governmental Dental College, Belgaum, for facilitating anti-TB assays and providing the procedure for the same.

References

[1] A. Koul, E. Arnoult, N. Lounis, J. Guillemont, K. Andries, The challenge of new drug discovery for tuberculosis, Nature 469 (2011) 483–490.
[2] R.C. Goldman, B.E. Laughon, Discovery and validation of new antitubercular compounds as potential drug leads and probes, Tuberculosis (Edinb) 89 (2009) 331–333.
[3] D. Murugesan, S. Palaniappan, Y. Perumal, C. Arnab, N. Valakunja, S. Dharmarajan, Bioorg. Med. Chem. 16 (2008) 3408–3418.
[4] L. Annamaria, M. Jialin, W. Baojie, W. Yuehong, G.F. Scott, P. K. Alan, J. Med. Chem. 52 (2009) 2109–2118.
[5] J. Sarva, I. Yasuyoshi, W. Baojie, G.F. Scott, P.K. Alan, Chem. Med. Chem. 1 (2006) 593–597.
[6] N. Amit, M. Vikramdeep, M. Alpeshkumar, C. Evans, J. Rahul, Bioorg. Med. Chem. 15 (2007) 626–640.
[7] M. Dinakaran, P. Senthilkumar, P. Yogeeswari, A. China, V. Nagaraja, S. Dharmarajan, Int. J. Antimicrob. Agents 31 (2008) 337–344.
[8] L. Savini, L. Chiasserini, A. Gaeta, C. Pellerano, Bioorg. Med. Chem. 10 (2002) 2193–2198.
[9] S. Eswaran, A.V. Adhikari, I.H. Chowdhury, N.K. Pal, K.D. Thomas, New quinoline derivatives: synthesis and investigation of antibacterial and antituberculosis properties, Eur. J. Med. Chem. 45 (2010) 3374–3383.
[10] E. Vavríkova, S. Polanc, M. Kocevar, K. Horvati, S. Bosze, J. Stolaríkova, et al, New fluorine-containing hydrazones active against MDR-tuberculosis, Eur. J. Med. Chem. 46 (2011) 4937–4945.
[11] S. Rollas, S.G. Küçükgüzel, Molecules 12 (2007) 1910–1939.
[12] S. Rao, D.D. Mishra, R.V. Mourya, N. Nageswara, Oxovanadium binuclear (IV) Schiff base complexes derived from aroyl hydrazones having subnormal magnetic moment, Polyhedron 16 (1997) 1825–1829.
[13] D.X. West, A.E. Liberta, S.B. Padhye, R.C. Chikate, P.B. Sonawane, A.S. Kumbhar, R.G. Yerande, Thiosemicarbazone complexes of copper(II): structural and biological studies, Coord. Chem. Rev. 123 (1993) 49–71.
[14] B.L. Vallee, D.S. Auld, Biochemistry 29 (1990) 5647.
[15] A.I. Bush, Curr. Opin. Chem. Biol. 4 (2000) 184.
[16] T.B. Cole, A. Martyanova, R.D. Palmiter, Brain Res. 891 (2001) 253.
[17] H. Tapiero, K.D. Tew, Biomed. Pharmacother. 57 (2003) 399.
[18] Z.H. Chohan, M.A. Farooq, Pak. J. Pharm. Sci. 7 (1994) 45.
[19] S. Eswaran, A.V. Adhikari, N.K. Pal, I.H. Chowdhury, Design and synthesis of some new quinoline-3-carbohydrazone derivatives as potential antimycobacterial agents, Bioorg. Med. Chem. Lett. 20 (2010) 1040–1044.
[20] K.D. Thomas, A.V. Adhikari, S. Telkar, I.H. Chowdhury, R. Mahmood, N.K. Pal, et al, Design, synthesis and docking studies of new quinoline-3-carbohydrazide derivatives as antitubercular agents, Eur. J. Med. Chem. 46 (2011) 5283–5292.
[21] M.C. Mandewale, B.R. Thorat, D. Shelke, R.S. Yamgar, Synthesis and biological evaluation of new hydrazone derivatives of quinoline and their Cu(II) and Zn(II) complexes against *Mycobacterium tuberculosis*, Bioinorg. Chem. Appl. 2015 (2015) 14, http://dx.doi.org/10.1155/2015/153015.
[22] M.C. Mandewale, B.R. Thorat, R.S. Yamgar, Synthesis and anti-mycobacterium study of some fluorine containing Schiff bases of quinoline and their metal complexes, Der Pharma Chem. 7 (2015) 207–215.
[23] O. Meth-Cohn, B. Narine, B. Tarnowski, A versatile new synthesis of quinolines and related fused pyridines. Part 5. The synthesis of 2-chloroquinoline-3-carbaldehydes, J. Chem. Soc. Perkin Trans. 1 (1981) 1520–1530.
[24] M. Mustapha, B.R. Thorat, S.S. Sawant, R.G. Atram, R.S. Yamgar, Synthesis of novel Schiff bases and its transition metal complexes, J. Chem. Pharm. Res. 3 (2011) 5–9.
[25] Ambika Shrivastav, R.M. Singh, Vilsmeier–Haack reagent: a facile synthesis of 2-chloro-3-formylquinoline from n-arylacetamides and transformation into different functionalities, Indian J. Chem. 44B (2005) 1868–1875.
[26] H.A. Bayoumi, M.A. Abdel-Nasser, Mutlak S.H. Aljahdali, Cu (II), Ni(II), Co(II) and Cr(III) complexes with N_2O_2-chelating Schiff's base ligand incorporating azo and sulfonamide moieties: spectroscopic, electrochemical behavior and thermal decomposition studies, Int. J. Electrochem. Sci. 8 (2013) 9399–9413.
[27] C.J. Dhanaraj, M.S. Nair, Synthesis, characterization, and antimicrobial studies of some Schiff-base metal(II) complexes, J. Coord. Chem. 62 (2009) 4018–4028.
[28] C.J. Dhanaraj, M.S. Nair, Synthesis and characterization of metal(II) complexes of poly(3-nitrobenzylidene-1-naphthylamineco-succinicanhydride), Eur. Polym. J. 45 (2009) 565–572.
[29] G.G. Mohamed, M.M. Omar, A.M. Hindy, Metal complexes of schiff bases: preparation characterization and biological activity, Turk. J. Chem. 30 (2006) 361–382.
[30] M.S. Lourenco, M.N. DeSouza, A.C. Pinheiro, M.L. Ferreira, R.B. Goncalves, T.M. Nogneira, M.A. Peralta, Evaluation of anti-tubercular activity of nicotinic and isoniazid analogues, ARKIVOC 15 (2007) 181–191.
[31] A.K. Kralova, K. Kissova, O. Svajlenova, J. Vanco, Biological activity of copper(II) N-salicylideneaminoacidato complexes. Reduction of chlorophyll content in freshwater alga *Chlorella vulgaris* and inhibition of photosynthetic electron transport in spinach chloroplasts, Chem. Pap. 58 (2004) 357–361.
[32] J. Parekh, P. Inamdhar, R. Nair, S. Baluja, S. Chanda, Synthesis and antibacterial activity of some Schiff bases derived from 4-aminobenzoic acid, J. Serb. Chem. Soc. 70 (2005) 1155–1161.
[33] Y. Vaghasia, R. Nair, M. Soni, S. Baluja, S. Chanda, Synthesis, structural determination and antibacterial activity of compounds derived from vanillin and 4-aminoantipyrine, J. Serb. Chem. Soc. 69 (2004) 991–998.

[34] N. Raman, Antibacterial study of the mannich base, N-(1-morpholino-benzyl) semicarbazide and its transition metal(II) complexes, Res. J. Chem. Environ. 4 (2005) 9.
[35] U. Galm, S. Heller, S. Shapiro, M. Page, S.M. Li, L. Heide, Antimicrobial and DNA gyrase-inhibitory activities of novel clorobiocin derivatives produced by mutasynthesis, Antimicrob. Agents Chemother. 48 (2004) 1307–1312.
[36] E.J. Alvarez, V.H. Vartanian, J.S. Brodbelt, Metal complexation reactions of quinolone antibiotics in a quadrupole ion trap, Anal. Chem. 69 (1997) 1147–1155.

Please cite this article in press as: M.C. Mandewale et al., Synthesis, structural studies and antituberculosis evaluation of new hydrazone derivatives of quinoline and their Zn(II) complexes, Journal of Saudi Chemical Society (2016), http://dx.doi.org/10.1016/j.jscs.2016.04.003